IMPEDANCE-BASED VENTILATION DETECTION DURING CARDIOPULMONARY RESUSCITATION USING A NEURAL NETWORK

M. Risdal*, M. Stavland**, S. O. Aase*, and T. Eftestøl*

*University of Stavanger, Stavanger, Norway
**Laerdal Medical AS, Stavanger, Norway

martin.risdal@uis.no

Abstract: To improve quality of cardiopulmonary resuscitation (CPR), it has been suggested to expand automated external defibrillators (AED) with the ability to monitor the CPR performance and give feedback for possible improvements online. Thoracic impedance (TI) changes are closely correlated to the lung volume changes and can be used to monitor the ventilatory activity. This calls for an accurate ventilation detection algorithm. A detection algorithm needs to discriminate between onset of inspiration (OI), onset of expiration (OE) and no onset (NO). We therefore wanted to evaluate a neural network's ability to discriminate between these three classes in realistic data from 20 cardiac arrest episodes. The classifier achieved a mean (standard deviation) area under the receiver operating characteristics curve (AUC) of 0.992 (0.009) when discriminating between OI and OE, 0.946 (0.035) when discriminating between OI and neither, and 0.970 (0.016) when discriminating between OE and neither. The results indicate a good potential for using classification with a neural network as basis for a ventilation detection algorithm.

Introduction

Recent publications [1, 2, 3] concerning CPR quality has shown high incidence of divergence from the recommendations of Guidelines 2000 [4]. The main problems are hyperventilation, wrong compression rates, too shallow compressions and long pauses in CPR. Animal studies have shown that hyperventilation markedly decrease survival rates [3]. Other studies indicate that the quality of CPR performance influences the outcome [5, 6, 7]. A possible way to ensure high quality of CPR, and thereby potentially increase survivability, is to use real time automated feedback for guiding personnel performing CPR. The use of automated feedback has shown positive results in manikin studies [8]. It has been suggested [9] to expand the automated external defibrillators (AED) with this kind of functionality. Improvements of the AED may also help reduce the pauses in CPR [10]. Compression monitoring can be done using the principles of inertia navigation and a chest compression sensor [11]. Transthoracic impedance (TI) change close to linearly with lung volume changes [12]. The TI can be monitored through the self-adhesive defibrillator pads, and be used for ventilation assessment [9, 13]. By analyzing the impedance signal resulting from a ventilation cycle, the AED can possibly give feedback on ventilation volume, inflation time and rate [13].

TI-based feedback is dependent on automatic detection of the ventilations. This is not an easy task in a CPR situation. The impedance measurement is very sensitive to movement of the patient, and chest compressions severely corrupt the signal. It also has a significant baseline drift, and the ventilatory-related curves may assume a wide range of amplitudes, durations and shape depending on the ventilatory efforts of the rescuer. The relationship between amount of air given to the patient and the resulting impedance change, is in addition different from person to person [14].

Thorax impedance is in use for monitoring of apnea, which also calls for an accurate detection algorithm. Sa et al proposed using two independent neural networks to identify windows of interest where the onset of inspiration and expiration occurs [15]. The minimum and maximum within these windows are then found to indicate onset of inspiration and expiration. We intend to use a similar approach, but instead of two neural networks we use one. The impedance signal measured by the AED during CPR is also much more unstable because of handling of the patient, and makes the task of detecting ventilations more difficult than in apnea monitoring. We therefore introduce the use of features characterizing the shape of the windowed signal, which are used as inputs to the neural network. The output of the neural network is used to classify the segment as either OI, OE or NO. This classifier will be the core of the ventilation detection system. We seek to evaluate such a classifier's ability to discriminate between the different classes before designing the entire detection system.

Materials and Methods

Data from 20 representative cardiac arrest episodes recorded during the data collection for the study presented in [2] forms the basis for the evaluation of the classifier. The episodes were analyzed using a custom-made computer program designed for the original study [2], and starts and tops of ventilation cycles were annotated manually. More details of the data set are presented in Table 1.

A modified Heartstart 4000 defibrillator (Laerdal Medical, Stavanger, Norway), HS4000SP, was used for the impedance measurements. A 32 kHz sinusoidal excitation current, 3mA peak-to-peak, was applied between the defibrillation pads, and the resulting impedance was registered. The resolution of the defibrillator impedance measurement system was 0.74 mΩ/bit. Sampling rate was 500 Hz and dynamic range was 16 bits. The defibrillation pads were of the type Heartstream external defibrillation pads (Philips Medical Systems, Seattle, WA, USA), and were placed in accordance with recommendations on AED usage [16].

A sliding window of N samples of the impedance signal $x(n)$ at time instant n is represented as

$$\mathbf{x}_{seg}(n) = [x(n-N+1), x(n-N+2), \ldots, x(n)]^T \quad (1)$$

We extract discriminating features $\mathbf{v}(n)$ from $\mathbf{x}_{seg}(n)$, and present them to the neural net. The output of the neural network is used for classification of the midpoint of the segment, $n - N/2$, as either OI, ω_1, OE, ω_2 or NO, ω_3.

Typical segments of the three classes are shown in Figure 1. A good representation of a segment should be able to reflect the distinctive shape of an inspiration or expiration onset. We therefore fit a polynomial to $\mathbf{x}_{seg}(n)$, and let the coefficients represent the windowed signal segment.

The mean of the segment is first subtracted from $\mathbf{x}_{seg}(n)$. The polynomial of order P that best fits $\mathbf{x}_{seg}(n)$ can then be found by solving

$$\mathbf{Ta} = \mathbf{x}_{seg}(n) \quad (2)$$

in a least squares sense, where

$$\mathbf{Ta} = \begin{bmatrix} 1 & t_1 & t_1^2 & \ldots & t_1^P \\ 1 & t_2 & t_2^2 & \ldots & t_2^P \\ \vdots & & & & \\ 1 & t_N & t_N^2 & \ldots & t_N^P \end{bmatrix} \begin{bmatrix} a_0 \\ a_1 \\ \vdots \\ a_P \end{bmatrix} \quad (3)$$

where $t_i = i - 1$ and a_i is the i'th coefficient of the fitted polynomial of degree P. A measure of how well the polynomial coefficients $\mathbf{a}$ represent $\mathbf{x}_{seg}(n)$ can be expressed as the mean squared error (MSE) between $\mathbf{Ta}$ and $\mathbf{x}_{seg}(n)$:

$$\text{MSE} = \frac{1}{N} \left(\mathbf{Ta} - \mathbf{x}_{seg}(n)\right)^T \left(\mathbf{Ta} - \mathbf{x}_{seg}(n)\right) \quad (4)$$

In order to find the best segment representation and choice of N, it is necessary to evaluate the alternatives with respect to discriminative power. For this purpose we construct a data set from the available episodes listed in Table 1, with the impedance signal being downsampled to 100 Hz. Only windows without compressions are used. We first assign all $\mathbf{x}_{seg}(n)$ with midpoint $n - N/2$ equal to the manually annotated OI to ω_1, and to ω_2 where $n - N/2$ is equal to the manually annotated OE. The remaining segments are assigned to ω_3. It is made sure that the distance between the midpoint of neighboring segments are at least 50 ms. 90 % of the segments assigned to ω_3 are randomly excluded from the data set to limit its size.

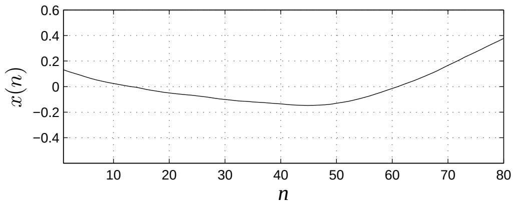

(a) $\mathbf{x}_{seg} \in \omega_1$.

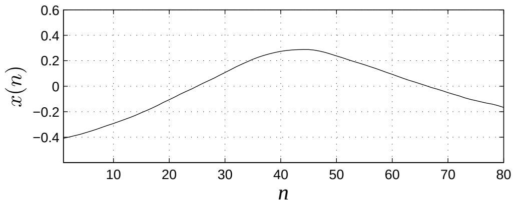

(b) $\mathbf{x}_{seg} \in \omega_2$.

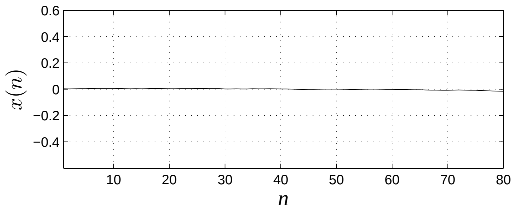

(c) $\mathbf{x}_{seg} \in \omega_3$.

Figure 1: Typical segments of the impedance trace of a ventilation.

We want to represent the segments using polynomial coefficients and the resulting MSE calculated from Eq. 4. By using the coefficients and MSE of polynomials of order 1, 2, 3 and 4, we have a total of 18 features. We impose the restriction of only using features that are not highly correlated. We compute the correlation coefficient ρ between all features. If $|\rho| > 0.9$ for two features derived from different polynomials, we use the feature from the polynomial of lowest order. If $|\rho| > 0.9$ for two features derived from the same polynomial, we use the feature of the

Table 1: The data material

Episode nr.	Duration (h:mm:ss)	# of vent.	Mean amp. [Ω]	Amp. range [Ω]	# of ventilations not during compressions
1	0:37:15	309	1.13	0.36-1.74	170
2	0:28:24	294	0.90	0.56-1.45	139
3	0:37:44	341	1.03	0.34-1.68	220
4	0:27:44	233	1.92	0.86-3.90	131
5	0:23:09	202	1.50	0.64-2.75	68
6	0:27:47	352	2.89	0.33-5.69	350
7	0:27:35	202	0.68	0.30-1.07	193
8	0:37:10	237	0.57	0.09-1.53	187
9	0:20:05	189	1.29	0.42-2.24	129
10	0:20:30	280	0.66	0.39-0.94	182
11	0:32:39	159	0.82	0.40-1.68	112
12	0:13:19	73	1.21	0.80-2.15	59
13	0:20:04	73	1.27	0.51-1.89	38
14	0:16:34	123	0.82	0.28-1.58	91
15	0:23:39	242	0.29	0.14-0.42	179
16	0:38:29	624	0.77	0.35-1.24	274
17	0:26:29	145	0.99	0.36-4.04	80
18	0:10:14	532	1.07	0.45-1.75	263
19	0:45:44	188	0.91	0.15-2.23	24
20	0:11:54	103	0.73	0.46-0.93	103

highest power. We use the remaining features to represent the segment.

The neural network consists of a variable number of inputs, depending on the length of $\mathbf{v}$, one hidden layer with a variable number of units and 3 output units, one for each class. The sigmoid function is used as transfer function between the layers. This gives outputs similar in value to probabilities. Learning is achieved using the resilient backpropagation algorithm [17]. Number of learning epochs is varied to reveal which gives the best performance. M-fold cross-validation [18] is then used to ensure separate training and test set, with $M = 5$. For each evaluation run, data from 19 episodes are used for training, and data from the remaining episode is used for testing.

The performance of a classifier can be evaluated and visualized by means of Receiver Operating Characteristics (ROC) graphs [18]. The area under the ROC curve, AUC, is used as a measure of performance, and gives a general measure of how well the classifier manages to discriminate between the classes. AUC is used because it is not influenced by the number of elements in each class, and our problem has substantially more data from class ω_3 than from ω_1 and ω_2. The technique is however only applicable to the case of two classes. A method for using AUC in the evaluation of multiple class classifiers was proposed in [19]. The multiple class problem is divided in all possible two-class problems, and the overall performance, AUC_{total}, is simply the mean AUC of the two-class problems. This is expressed as

$$\text{AUC}_{total} = \frac{2}{c(c-1)} \sum_{i<j} \text{AUC}_{i,j} \tag{5}$$

where c is the total number of classes and $\text{AUC}_{i,j}$ is the area under the ROC curve when discriminating between elements from class ω_i and ω_j. The original 3-class problem is therefore divided in three 2-class problems. This will also give us more detailed information about the performance of the classifier. We then need to estimate ROC graphs. We treat output i of the neural network as the discriminant function $g_i(\mathbf{v})$ of observing $\mathbf{v}$. The decision rule for minimizing the overall risk for a two-category classification problem is to assign the observation to class ω_1 if

$$(\lambda_{21} - \lambda_{11}) \cdot g_1(\mathbf{v}) > (\lambda_{12} - \lambda_{22}) \cdot g_2(\mathbf{v}) \tag{6}$$

and otherwise assign it to ω_2 [18]. λ_{ij} is the cost of deciding that $\mathbf{v} \in \omega_i$, when in fact $\mathbf{v} \in \omega_j$. By adjusting the costs, we can get $(\lambda_{ji} - \lambda_{ii})g_i(\mathbf{v})$ to assume any value we want. We let $(\lambda_{21} - \lambda_{11}) = c_1$ and $(\lambda_{12} - \lambda_{22}) = c_2$, and reformulate the decision rule to assign the observation to class ω_1 if

$$c_1 \cdot g_1(\mathbf{v}) > c_2 \cdot g_2(\mathbf{v}) \tag{7}$$

and otherwise assign it to ω_2. For a choice of c_1 and c_2 we can now calculate the sensitivity and specificity [20] of our training and test set, and thereby points on the ROC graph. For implementation purposes we impose the restriction of $c_1 + c_2 = 1$, and let $c_1 \in [0, 0.001, \ldots, 0.999, 1]$ to compute points on the ROC graphs. The area under the ROC graph, AUC, can then be calculated for each test set. The estimate of the classifier's performance is then calculated as the mean of the AUC over all test sets, which gives a general measure of the classifier's performance. The standard deviation is also calculated to get an impression of the generality of the classifier.

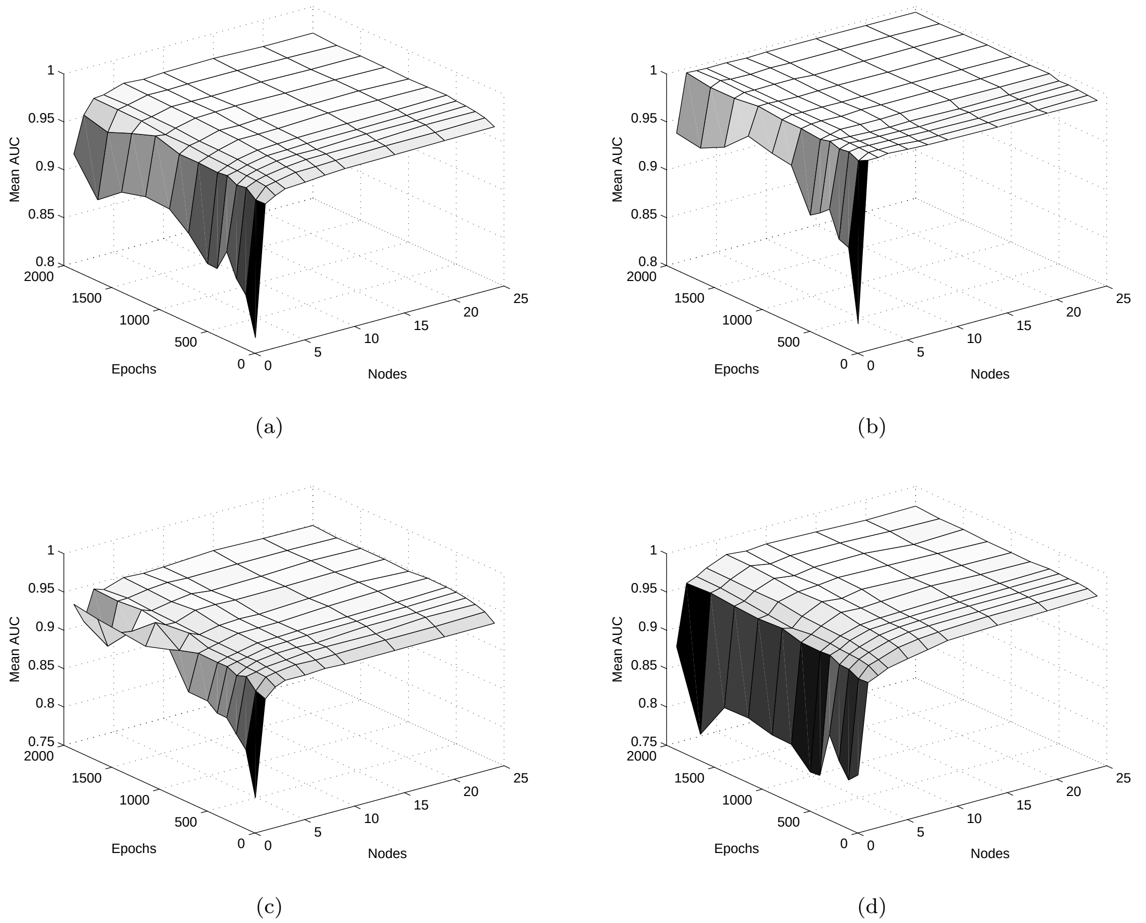

Figure 2: The mean (a) AUC_{total}, (b) $\mathrm{AUC}_{1,2}$, (c) $\mathrm{AUC}_{1,3}$ and (d) $\mathrm{AUC}_{2,3}$ of the classifier for different neural network architectures.

We first find the feature vector with low correlation ($|\rho| < 0.9$) between the features for window lengths of 500 ms, 1000 ms and 1500 ms. We then evaluate the performance of a neural network with 5 hidden nodes and 200 training epochs for window lengths from 500 to 1500 ms, with steps of 100 ms. This is done to find a good choice of N. Using the window length that gives the best discrimination, we evaluate the performance of the classifier when increasing the number of hidden nodes and training epochs to see if the performance diverges.

Results

A feature vector which satisfied our demand on correlation between features was found to be

$$\mathbf{v} = [a_1^{(1)}, MSE^{(1)}, a_2^{(2)}, a_0^{(2)}, a_3^{(3)}, a_1^{(4)}, a_1^{(4)}]^T \quad (8)$$

where $a_i^{(P)}$ is the i'th coefficient of the polynomial of order p that best represents the segment (see Eq. 3), and $MSE^{(P)}$ is the error of the fitted polynomial of order P (see Eq. 4). This feature vector was used to represent the windowed segments. The results of the evaluation of the window length's influence on performance is presented in Figure 3. The best

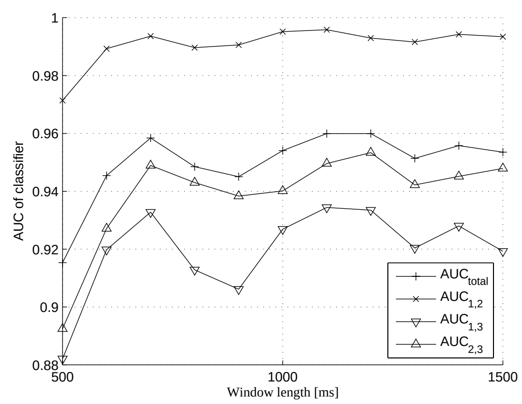

Figure 3: The mean AUC of the neural network for different window lengths.

overall performance is achieved for window lengths of 1.1 seconds, and is therefore used in the evaluation of different neural network architectures. It is worth noticing that very good results also are achieved for a window length of 0.7 seconds, which would give a smaller delay in real-time detection.

The performance of the classifier for different

ISSN: 1727-1983 © 2005 IFMBE

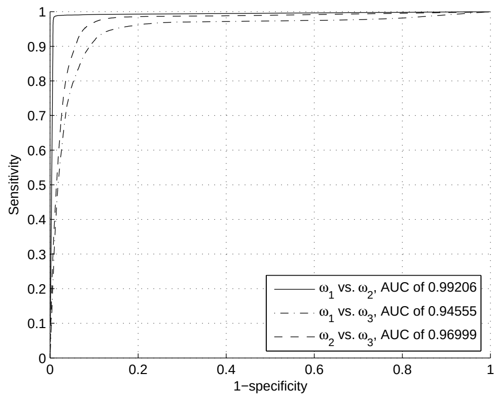

Figure 4: The ROC curves of a neural network with 5 hidden nodes and 1000 training epochs for the three tasks of discriminating between ω_1 and ω_2, between ω_1 and ω_3, and between ω_2 and ω_3.

number of hidden nodes and training epochs can be seen in Figure 2. As the complexity and the number of training epochs increased, the performance of the classifier diverged toward $\mathrm{AUC}_{1,2} = 0.99$, $\mathrm{AUC}_{1,3} = 0.95$ and $\mathrm{AUC}_{2,3} = 0.97$. The ROC curves of a classifier with 5 hidden nodes and 1000 training epochs are shown in Figure 4.

Discussion & Conclusion

The use of a neural network for discriminating between onset of inspiration, onset of expiration and neither shows great potential as basis for an impedance-based ventilation detection algorithm. Using the results in Figure 4, the neural network can be tuned to correctly classifying 95 % of the data being an onset of expiration, with the effect of wrongful classifying 10 % of the no onset data. In a system for ventilation detection, the erroneous recognitions can be reduced by requiring OI and OE to appear in pairs within certain limits in time and amplitude. The limits can be set based on training data.

One potential problem with the idea of using a neural network in a detection system is the computational complexity. The system design will be a balance between complexity and performance. Increasing complexity will introduce an increasing delay of the detection system, and make it less useable in a real-world setting. The features representing the windowed segments should therefore require as few computations as possible, and the number of nodes in the neural network should be kept at a minimum. From Figure 2 it can be seen that good performance can be achieved with a low number of hidden nodes if the neural net is sufficiently trained. In addition the use of windows will introduce a delay. In order to classify time instant n as an OI, OE, or neither, the classifier has to have knowledge of the impedance signal from $n - N/2$ to $n + N/2$. This introduces a delay of $N/2$ before a classification can be made.

Future research should include an evaluation of any benefits in performance from low pass filtering the windowed segments before presenting them to the neural network. Respiration artifacts are low frequency in nature, and their features may potentially be enhanced by filtration. Because of this, downsampling may therefore help reduce the complexity without affecting the performance. The performance should also be evaluated when used in combination with a compression-artefact filter [21] during compressions.

References

[1] ABELLA B. S., ALVARADO J. P., MYKLEBUST H., EDELSON D. P., BARRY A., O'HEARN N., VANDEN HOEK T. L., and BECKER L. B.(2005): 'Quality of cardiopulmonary resuscitation during in-hospital cardiac arrest', *JAMA*, **293**(3), pp. 305–310

[2] WIK L., KRAMER-JOHANSEN J., MYKLEBUST H., SØREBØE H., SVENDSEN L., FELLOWS B., and STEEN P. A. (2005): 'Quality of cardiopulmonary resuscitation during out-of-hospital cardiac arrest', *JAMA*, **293**(3), pp. 299–304

[3] AUFDERHEIDE T. P., SIGURDSSON G., PIRRALLO R. G., YANNOPOULOS D., MCKNITE S., VON BRIESEN C., SPARKS C. W., CONRAD C. J., PROVO T. A., and LURIE K. G. (2004): 'Hyperventilation-induced hypotension during cardiopulmonary resuscitation', *Circulation*, **109**(16), pp. 1960–1965

[4] 'Guidelines 2000 for cardiopulmonary resuscitation and emergency cardiovascular care: international consensus on science', *Circulation*, **102** (suppl I), 2000.

[5] WIK L., STEEN P. A., and BIRCHER N. G. (1994): 'Quality of bystander cardiopulmonary resuscitation influences outcome after prehospital cardiac arrest', *Resuscitation*, **28**, pp. 195–203

[6] VAN HOEYWEGHEN R. J., BOSSAERT L. L., and MULLIE A. (1993): 'Belgian cerebral resuscitation study group. Quality and efficiency of bystander CPR', *Resuscitation*, **26**, pp. 47–52

[7] GALLAGHER E. J., LOMARDI G., and GENNIS P. (1995): 'Effectiveness of bystander cardiopulmonary resuscitation and survival following out-of-hospital cardiac arrest', *JAMA*, **274**, pp. 1922–1925

[8] WIK L., THOWSEN J., and STEEN P. A. (2001): 'An automated voice advisory manikin system for training in basic life support without an instructor. A novel approach to CPR training', *Resuscitation*, **50**, pp. 167–172

[9] PELLIS T., BISERA J., TANG W., and WEIL M. H. (2002): 'Expanding automatic external defibrillators to include automated detection of cardiac, respiratory, and cardiorespiratory arrest'. *Crit Care Med.*, **30**

[10] EILEVSTJØNN J., KRAMER-JOHANSEN J., EFTESTØL T., STAVLAND M., MYKLEBUST H., and STEEN P. A. (2005): 'Reducing no flow times during automated external defibrillation'. *Resuscitation*, In press.

[11] AASE S. O. and MYKLEBUST H. (2002): 'Compression depth estimation for CPR quality assessment using DSP on accelerometer signals', *IEEE Transactions on Medical Engineering*, **49**(3), pp.263–268

[12] BAKER, L. E. and GEDDES, L. A. (1989): '*Principles of Applied Biomedical Instrumentation*', Wiley-Interscience, 3rd edition

[13] RISDAL M., LOSERT H., NYSÆTHER J., AASE S. O., STERZ F., and EFTESTØL T. (2005): 'Non-invasive ventilation monitoring during cardiopulmonaryresuscitation by means of thoracic impedance', In *Proceedings of 3rd Eurpean Medical & Biological Engineering Conference*

[14] VALENTINUZZI M. E., MORUCCI J. P., and FELICE C. J. (1996): 'Bioelectrical impedance techniques in medicine. part II: Monitoring of physiological events by impedance', *Crit Rev Biomed Eng*, **24**, pp. 353–466

[15] SA R. C. and VERBANDT Y. (2002): 'Automated breath detection on long-duration signals using feedforward backpropagation artificial neural networks', *IEEE Transactions on Biomedical Engineering*, **49**(10), pp. 1130 – 1141

[16] 'Guidelines 2000 for cardiopulmonary resuscitation and emergency cardiovascular care. part 4: The automated external defibrillator' *Circulation*, **102** (suppl I), 2000

[17] RIEDMILLER M. and BRAUN H. (1993): 'A direct adaptive method for faster backpropagation learning: The RPROP algorithm', Proc. of IEEE Int. Conf. on Neural Networks 1993, **1**, pp. 586 – 591

[18] DUDA, R. O., HART, P. E., and STORK, D. G. (2000): 'Pattern Classification', Wiley-Interscience, 2nd edition

[19] HAND D. J. and TILL R. J. (2001): 'A simple generalisation of the area under the ROC curve for multiple class classification problems', *Machine Learning*, **45**, pp. 171–186

[20] RANGAYYAN, R. M. (2002): 'Biomedical Signal Analysis', Wiley-Interscience

[21] HUSØY J. H., EILEVSTJØNN J., EFTESTØL T., AASE S. O., MYKLEBUST H., and STEEN P. A. (2002): 'Removal of cardiopulmonary resuscitation artifacts from human ECG using an efficient matching pursuit-like algorithm', *IEEE Trans. Biomedical Engineering*, **49**(11), pp. 1287–1298

ISSN: 1727-1983 © 2005 IFMBE